

# MR Elastography for the Assessment of Hepatic Fibrosis in Patients with Chronic Hepatitis B Infection: Does Histologic Necroinflammation Influence the Measurement of Hepatic Stiffness?<sup>1</sup>

Yu Shi, MS  
 Qiyong Guo, MD  
 Fei Xia, MS  
 Bogdan Dzyubak, BS  
 Kevin J. Glaser, PhD  
 Qiuju Li, BS  
 Jiahui Li, BS  
 Richard L. Ehman, MD

<sup>1</sup>From the Departments of Radiology (Y.S., Q.G., Q.L., J.L.) and Infectious Disease (F.X.), Shengjing Hospital, China Medical University, 36 Sanhao St, Heping District, Shenyang 110004, People's Republic of China; and Departments of Biomedical Engineering (B.D.) and Radiology (K.J.G., R.L.E.), Mayo Clinic, Rochester, Minn. Received November 8, 2013; revision requested December 26; revision received February 9, 2014; accepted March 10; final version accepted March 21. Supported by the National Natural Science Foundation of China (grants 81071123 and 81271566). Address correspondence to Q.G. (e-mail: [guoqiyongcmu@163.com](mailto:guoqiyongcmu@163.com)).

© RSNA, 2014

## Purpose:

To determine the diagnostic performance of magnetic resonance (MR) elastography for the staging of hepatic fibrosis and to evaluate the influence of necroinflammation on hepatic stiffness in patients with chronic hepatitis B virus (HBV) infection by using histopathologic findings as the reference standard.

## Materials and Methods:

One hundred thirteen consecutive patients with chronic HBV infection were recruited prospectively in this institutional review board–approved study after providing written informed consent between March 2012 and October 2013. The stiffness measurements were obtained by using two-dimensional gradient-echo MR elastography with a 3.0-T MR system. The METAVIR scoring system was used for the assessment of fibrosis (“F” stage) and necroinflammation (“A” grade). The predictive ability of MR elastography was evaluated by using the receiver operating characteristic (ROC) curve and the area under the ROC curve (AUC). Multiple linear regression analyses were conducted to determine the relationship between hepatic stiffness and the variables that showed a significant association in the univariate analysis or those that were of interest for comparison with earlier work (histologic scores, sex, age, aspartate aminotransferase level, and aspartate aminotransferase/alanine aminotransferase ratio).

## Results:

MR elastography showed excellent performance for characterization of  $\geq F1$ ,  $\geq F2$ ,  $\geq F3$ , and F4 findings, with AUC values of 0.961, 0.986, 1.000, and 0.998, respectively. It showed a moderate capability for evaluation of necroinflammatory activity of  $\geq A1$ ,  $\geq A2$ , and A3 (AUC = 0.806, 0.834, and 0.906, respectively). Multiple linear regression analysis showed that fibrosis, necroinflammation, and sex were independently associated with hepatic stiffness ( $\beta = 0.799, 0.277, \text{ and } 0.070$ , respectively;  $P < .05$ ). For pairwise comparisons, log-transformed hepatic stiffness showed no difference between (a) groups F0/A2–3 and F1/A0–1 and (b) groups F1/A2–3 and F2/A0–1 ( $P > .99$  and  $P = .486$ , respectively).

## Conclusion:

MR elastography demonstrated excellent performance for distinguishing the stages of hepatic fibrosis in patients with chronic HBV infection. For hepatic tissue with  $\leq F2$  fibrosis, necroinflammation can account for a substantial fraction of the increase in hepatic stiffness.

© RSNA, 2014

According to the World Health Organization, more than 240 million people have a chronic hepatitis B virus (HBV) infection (1), 185 million people have chronic hepatitis C virus (HCV) infection, and an additional 3 to 4 million people are infected each year (2). HBV and HCV infections are prevalent throughout the world, and their consequences can be serious (3,4). Long-term chronic infection with one or both of these viruses is the most common cause of hepatic fibrosis, leading to hepatic cirrhosis and hepatocellular carcinoma (5,6).

Chronic HBV infection is different from chronic HCV infection in both clinical course and histologic changes (7,8). Chronic HBV infection displays a fluctuating pattern of hepatic inflammation and fibrosis progression characterized by recurrent episodes of abnormal hepatic function, whereas chronic HCV has a more severe and continuous progressive course (7). In a prior study, hepatic tissue with pathologically proven inflammation but without any fibrosis showed a mild elevated stiffness by using magnetic resonance (MR) elastography and comparing the findings with those of healthy hepatic tissues (9). Moreover,

other studies have demonstrated histologic differences between chronic HCV and chronic HBV fibrotic patterns, noting higher perisinusoidal fibrosis in chronic HCV infection for patients with a fibrosis stage ("F" stage) of  $\leq$ F2 (8). Hence, when comparing hepatic tissue with the same severity of fibrosis shown by histopathologic findings in patients with chronic HCV and chronic HBV infections, chronic HBV-infected tissue might have less collagen and more variable inflammatory changes than tissue with chronic HCV infection.

MR elastography is increasingly being used clinically as a noninvasive method to stage hepatic fibrosis (10–25). However, MR elastography studies in patients with homogeneous HBV infection or direct comparative studies between HBV and HCV are rare (26–29). Studies involving the use of transient elastography have shown that it is not accurate for physicians to apply the same stiffness cutoff values determined in patients with chronic HCV infection to the population with chronic HBV infection for evaluation of hepatic fibrosis (7,30). Likewise, the cutoff stiffness values for MR elastography that optimize the sensitivity and specificity in chronic HCV infection might cause over- or underestimation of the real fibrotic status in chronic HBV infection (10,15,16,31,32). Hence, the aim of this study was to determine the diagnostic performance of MR elastography for the staging of hepatic fibrosis and evaluate the influence of necroinflammation on hepatic stiffness in patients with chronic HBV infection by using histopathologic findings as the reference standard.

### Advances in Knowledge

- MR elastography had high diagnostic accuracy for hepatic fibrosis in chronic hepatitis B virus (HBV) infection, with an area under the receiver operating characteristic curve of 0.961, 0.986, 1.000, and 0.998 for fibrosis stages F1, F2, F3, and F4, respectively.
- Both fibrosis stage and necroinflammation grade were independent factors that contributed to hepatic stiffness (multivariate linear regression,  $\beta = 0.799$  and  $0.277$ , respectively;  $P < .001$ ).
- The variable contribution of necroinflammation to hepatic stiffness can be a confounding factor that can cause overestimation of nonadvanced fibrosis (fibrosis stage  $\leq 2$ ).

### Implication for Patient Care



- The results indicate that MR elastography is suitable for stratifying patients with hepatic fibrosis caused by chronic HBV infection; for hepatic tissue with  $\leq$ F2 fibrosis, necroinflammation accounts for a portion of the elevated hepatic stiffness.

## Materials and Methods

### Patients

This prospective study was approved by our institutional review board, and written informed consent for the study was obtained. The Mayo Clinic and two authors (K.J.G. and R.L.E.) have intellectual property rights and a financial interest in MR elastography. Y.S. and Q.G. had control of the data. Between March 2012 and October 2013, 173 consecutive Asian patients with chronic HBV infection referred to the division of infectious diseases of our Asian hospital for medical treatment were initially included in the study if (a) they were 18 years old or older without known or recent pregnancy, (b) they planned to undergo a biopsy during their hospitalization or underwent histologic examination within 3 months of hospitalization, (c) they had HBV surface antigen for more than 6 months and serum HBV DNA levels higher than  $10^5$  copies per milliliter or persistent or intermittent increase in

Published online before print

10.1148/radiol.14132592 Content codes:  

Radiology 2014; 273:88–98

### Abbreviations:

ALT = alanine aminotransferase  
 AST = aspartate aminotransferase  
 AUC = area under the ROC curve  
 BMI = body mass index  
 CI = confidence interval  
 HBV = hepatitis B virus  
 HCV = hepatitis C virus  
 IQR = interquartile range  
 ROC = receiver operating characteristic  
 ROI = region of interest

### Author contributions:

Guarantors of integrity of entire study, Y.S., Q.G.; study concepts/study design or data acquisition or data analysis/interpretation, all authors; manuscript drafting or manuscript revision for important intellectual content, all authors; approval of final version of submitted manuscript, all authors; literature research, Y.S., F.X., K.J.G., Q.L., J.L.; clinical studies, Y.S., Q.G., F.X., K.J.G., Q.L., J.L.; experimental studies, K.J.G., R.L.E.; statistical analysis, Y.S., Q.L., J.L.; and manuscript editing, Y.S., Q.G., F.X., B.D., K.J.G., R.L.E.

### Funding:

This research was supported by the National Institutes of Health (grant EB001981).

Conflicts of interest are listed at the end of this article.

Figure 1

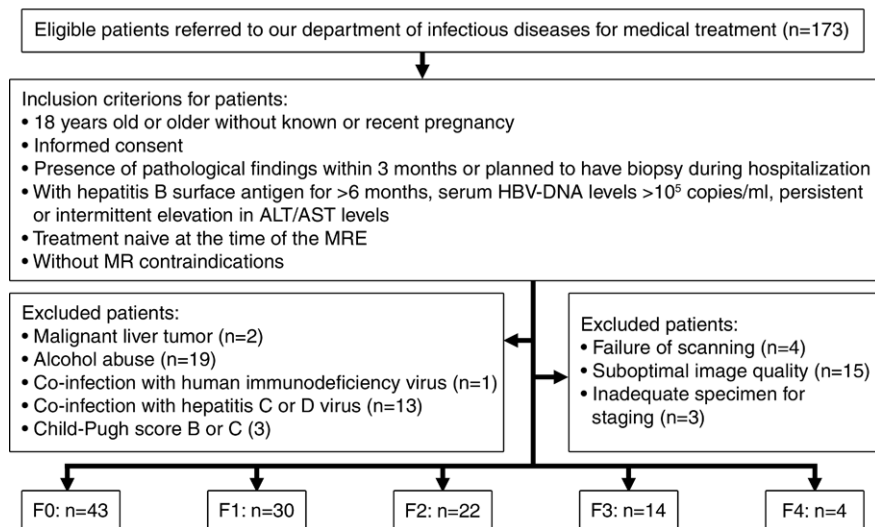


**Figure 1:** Flowchart shows the study enrollment process during the 19-month study period. “Treatment naive” indicates that no antiviral or other hepatic disease–related therapy was administered. MRE = MR elastography.

alanine aminotransferase (ALT) and/or aspartate aminotransferase (AST) levels, (d) they were patients who had not undergone antiviral or other hepatic disease–related therapy, and (e) they did not have any MR imaging contraindications. Patients were excluded if they had (a) other causes of chronic hepatic disease (eg, hepatitis C or D virus, excessive alcohol consumption [more than 30 g per day], hemochromatosis, autoimmune hepatitis, Wilson disease,  $\alpha_1$ -antitrypsin deficiency, primary sclerosing cholangitis, or primary biliary cirrhosis), (b) human immunodeficiency virus coinfection or hepatitis C or D coinfection, (c) a hepatic tumor that interfered with effective hepatic stiffness measurements, (d) hepatic decompensation—Child-Pugh score higher than 6 (class B and C), or (e) imaging complications (eg, operator error or driver problems while performing the examination, failure to perform the necessary breath holds, or too little liver considered to be able to achieve valid stiffness estimates with the inversion and region of interest [ROI] placement algorithms). One hundred thirteen patients were ultimately included in this study on the basis of these selection criteria (Fig 1). Patients ranged

in age from 19 to 62 years (median age, 42 years) and included 48 men and 65 women. The median patient age was 43 years (25th to 75th percentile of the interquartile range [IQR], 34–47 years) for men and 42 years (IQR, 35–47 years) for women ( $P = .466$ ). The median body mass index (BMI) was 21.71 kg/m<sup>2</sup> (range, 17.8–32.6 kg/m<sup>2</sup>). The median BMI was 21.43 kg/m<sup>2</sup> for men (IQR, 19.21–24.43 kg/m<sup>2</sup>) and 22.49 kg/m<sup>2</sup> for women (IQR, 20.95–24.91 kg/m<sup>2</sup>) ( $P = .008$ ). A fasting venous blood sample was acquired to measure the ALT and AST levels.

### MR Acquisitions

The participants were asked to fast for at least 6 hours prior to the examination. Each subject underwent MR elastography with a 3.0-T MR system (Signa Excite HD; GE Medical Systems, Milwaukee, Wis), equipped with an eight-element torso phased-array coil. Axial sections were acquired by using a two-dimensional gradient-echo MR elastography sequence. An active acoustic driver was located outside of the imaging room and generated 60-Hz mechanical vibrations. The active driver was connected via flexible tubing to a passive driver 19 cm

in diameter to deliver the vibrations to the right side of the subject’s rib cage. Both drivers were developed by the Mayo Clinic (Rochester, Minn) and were given to our institute along with a service agreement. Owing to imager updates, the MR elastography imaging parameters were different for some subjects. Forty-two patients underwent imaging while the system was using software version 15, and 71 patients underwent imaging after the system was upgraded to version 16. The MR elastography acquisition parameters for the 42 patients included repetition time (msec)/echo time (msec), 50/27.9; phase offsets, four; acquisition matrix size, 256 × 192; parallel imaging acceleration factor, two; flip angle, 30°; section thickness, 10 mm; fractional phase field of view, 0.7; and field of view, 34–40 cm, adjusted to body habitus. The MR elastography acquisition parameters for the 71 patients included 50/24.0; phase offsets, four; acquisition matrix size, 256 × 64; parallel imaging acceleration factor, two; flip angle, 30°; section thickness, 7 mm; fractional phase field of view, 1.0; and field of view, 34–40 cm, adjusted to body habitus. Each section was obtained in one breath hold of 28 seconds (14 seconds) at the end of expiration. There was no significant difference in the age ( $P = .498$ ) or sex ( $P = .922$ ) distribution in these two groups. The patient data from these two groups were pooled, as there were not enough subjects in each group for a robust statistical analysis and because the vibration frequency, stiffness estimation algorithm, and ROI definition techniques were kept constant.

### Measurement of Hepatic Stiffness

The MR elastography stiffness images were calculated from the acquired wave images by using an algorithm developed at and provided by Mayo Clinic that directly solves the Helmholtz wave equation with four two-dimensional directional filters (radial Butterworth bandpass filter cutoff frequencies of two and 128 cycles per field of view) (33–35). The shear stiffness of the tissue, in kilopascals, was

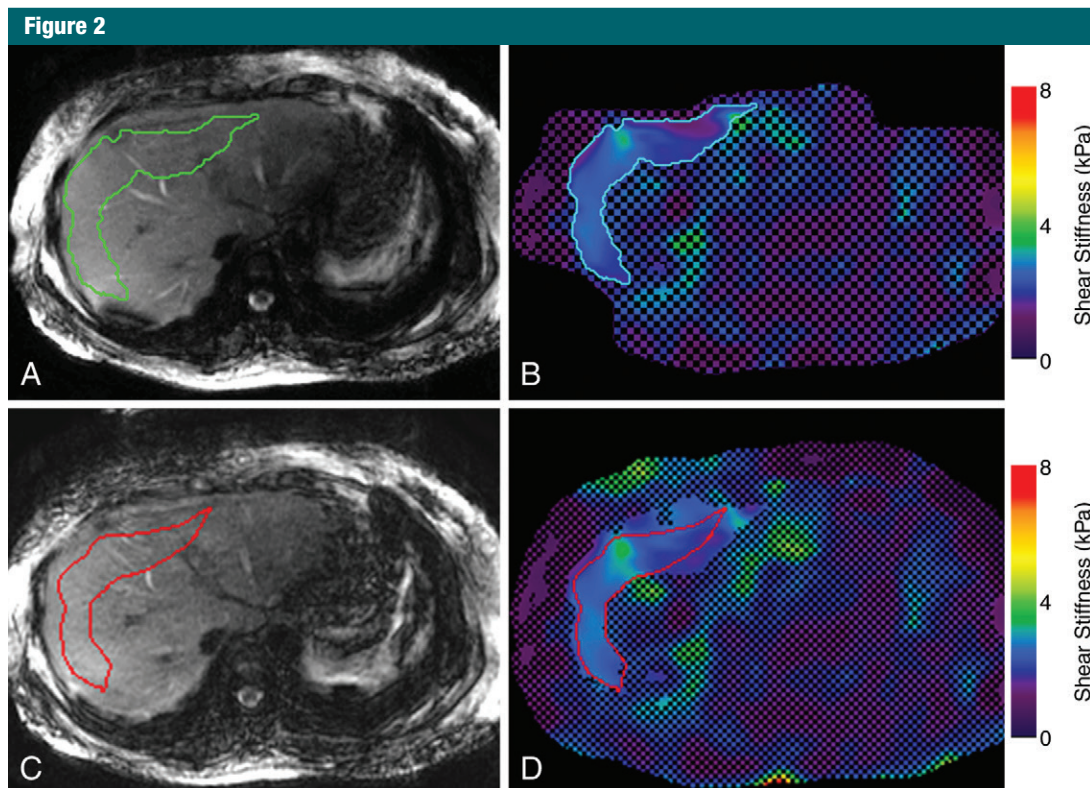


**Figure 2:** MR elastography magnitude images (left) and MR elastograms (right) in a 30-year-old man with fibrosis stage F0 and necroinflammation grade A1. *A*, Green outlined area indicates the automated ROI. *B*, Corresponding axial elastogram shows the same automated ROI. The recorded stiffness was  $2.26 \text{ kPa} \pm 0.29$ . *C*, Red outlined area indicates the reader-defined ROI, excluding areas of interference, portal areas, and blood vessels. *D*, Reader-defined ROI is shown on the elastogram, and the reported stiffness was  $2.34 \text{ kPa} \pm 0.19$ .

determined at each pixel and shown on an elastogram. The MR elastography wave, stiffness, and anatomic images were analyzed by using an in-house, fully automated algorithm for hepatic stiffness measurements described by Dzyubak et al (35). The ROI and the mean stiffness were automatically generated for all 113 patients (mean ROI size,  $2906 \text{ pixels} \pm 1393$ ; range, 1011–6222 pixels). If the ROI contained less than 1000 pixels, the image quality was considered suboptimal, and the subject was excluded from further analysis. Images acquired in 30 randomly selected patients, ranging in status from healthy to having severe fibrosis, were also analyzed by a human reader to confirm the reliability of the automated algorithm. The reader, who was blinded to the results from the automated processing (Y.S., with 7 years

of experience in abdominal diagnostic radiology and 2 years of experience with MR elastography measurements), measured the hepatic stiffness independently by creating ROIs manually by using the MR elastography magnitude, wave, and stiffness images according to the criteria discussed by Shire et al and Dzyubak et al (29,35). Figure 2 shows a representative example of the two measurements in one patient.

#### Assessment of Pathologic Specimens

Liver histologic examination was conducted semiquantitatively in percutaneous hepatic biopsy samples by using a 16-gauge disposable needle. The specimens were stained with hematoxylin-eosin and reviewed independently by two pathologists (two nonauthors with 14 and 18 years of experience and subspecialty expertise in hepatic pathology).

The pathologists were blinded to the clinical and imaging data. Hepatic biopsies that contained fewer than 11 portal tracts (except for cirrhosis) were excluded from the histologic analysis. The length of each hepatic biopsy specimen was measured in millimeters. Hepatic steatosis was expressed as the percentage of cells that contained fat vacuoles. The fibrosis stage and the necroinflammatory activity grade (“A” grade) were evaluated by using the METAVIR scoring system (36–38). Fibrosis was graded on a scale of 0 to 4 as follows: no fibrosis (F0); mild fibrosis, portal fibrosis without septa (F1); substantial fibrosis, portal fibrosis, and few septa (F2); advanced fibrosis, numerous septa without cirrhosis (F3); and cirrhosis (F4). The necroinflammatory activity score was graded on a scale of 0 to 3 as follows: no activity (A0), mild

activity (A1), moderate activity (A2), and severe activity (A3).

### Statistical Analysis

The stiffness values of the two independent measurements (the reader and the automated algorithm) were compared with both the Bland-Altman method (39,40) and the intraclass correlation coefficient. Agreement between the two pathologists was assessed with linearly weighted  $\kappa$  statistics for categorical variables. The level of agreement was defined as follows:  $\kappa = 0$ –0.20, poor agreement;  $\kappa = 0.21$ –0.40, fair agreement;  $\kappa = 0.41$ –0.60, moderate agreement;  $\kappa = 0.61$ –0.80, good agreement; and  $\kappa = 0.81$ –1.00, very good agreement (41). After calculating the  $\kappa$  values, any case in which the final fibrosis or inflammation grade differed between the two pathologists was re-evaluated and scored simultaneously by using a multipipe microscope to reach a consensus decision, or it was resolved in the presence of another senior pathologist (a nonauthor with 20 years of experience in hepatic pathology). The Spearman rank correlation coefficient was used to show the correlation between histologic scores and ALT, AST, AST/ALT ratio, and hepatic steatosis.

A receiver operating characteristic (ROC) curve analysis was used to evaluate the diagnostic performance of stiffness for fibrosis stage and necroinflammation grade by using the METAVIR scoring system as a reference standard, according to hepatic biopsy results. The area under the ROC curve (AUC) was used to evaluate the following classifications: F0 versus F1–F4 (stage  $\geq$ F1), F0 and F1 versus F2–F4 (stage  $\geq$ F2), F0–F2 versus F3 and F4 (stage  $\geq$ F3), F0–F3 versus F4 (stage F4), A0 versus A1–A3 (grade  $\geq$ A1), A0 and A1 versus A2 (grade  $\geq$ A2), and A3 activity (grade A3). Sensitivity, specificity, negative predictive value, and positive predictive value were calculated for the best stiffness threshold (as determined with the Youden index) to distinguish between different pathologic stages (42,43). Additionally, the AUC for prediction of fibrosis stage was further calculated according to different

necroinflammation grade (A2–A3 vs A0–A1). The Bayes theorem was used in the calculations by using the estimate of prevalence based on the database at our hospital with biopsy results for 1752 patients with HBV. The prevalence for  $\geq$ F1,  $\geq$ F2,  $\geq$ F3, and F4 was 75.20%, 57.80%, 41.80%, and 21.50% and for  $\geq$ A1,  $\geq$ A2, and A3 was 73.20%, 45.50%, and 14.60%, respectively.

Multiple linear regression with stepwise selection of variables was performed to evaluate the relationship of log stiffness and possible variables (fibrosis stage, necroinflammation grade, steatosis, sex, age, BMI, ALT, AST, and AST/ALT ratio) by showing a significant association in the univariate analysis (the relationship between variables [fibrosis stage, necroinflammation grade, age, AST, and AST/ALT ratio] with stiffness measures was described by using Pearson correlation coefficients and the *t* test [sex] or for comparison with earlier work).

Considering both the distribution of stiffness according to fibrosis and inflammation and the small number of subjects in each subgroup, the subjects with stage F3 and F4 fibrosis were further grouped together into the advanced fibrosis stage, and the A0–1/A2–3 subjects were grouped within each fibrotic stage, resulting in eight different pathologic groups: F0/A0–1, F0/A2–3, F1/A0–1, F1/A2–3, F2/A0–1, F2/A2–3, F3–4/A0–1, and F3–4/A2–3. One-way analysis of variance followed by the Bonferroni post hoc comparison test was performed to compare the means among these pathologic groups and between each pairwise group (after testing for normality with the Shapiro-Wilk test and testing for homogeneity of variance with the Levene test). Mann-Whitney *U* tests were used to compare the differences in ALT and AST between each pairwise pathologic group (Bonferroni correction,  $P < .0018$  [0.05/28]) and the age and BMI of men and women ( $P < .05$ ), since these data were not normally distributed.

All analyses were performed with Medcalc Version 7.4.2.0 statistical software (Medcalc Software, Mariakerke, Belgium) and SPSS Version 16.0 J

**Table 1**

### Distribution of Various Stages of Fibrosis and Grades of Necroinflammatory Activity according to the METAVIR Scoring System

Fibrosis Stage	Necroinflammatory Activity				Total
	A0	A1	A2	A3	
F0	8	22	13	0	43
F1	5	7	14	4	30
F2	0	9	6	7	22
F3	0	6	4	4	14
F4	0	0	1	3	4
Total	13	44	38	18	113

Note.—Data are number of patients.

(SPSS, Chicago, Ill). A *P* value less than .05 was considered to indicate a significant difference. When the Bonferroni correction was used to adjust for multiple comparisons, the *P* value was divided by the number of comparisons.

## Results

### Liver Histologic Findings

The mean biopsy length was 14 mm  $\pm$  7 (range, 4–26 mm). There was good agreement between the two independent pathologists with regard to fibrosis stage ( $\kappa = 0.76$ ; 95% confidence interval [CI]: 0.62, 0.90) and inflammatory activity grade ( $\kappa = 0.74$ ; 95% CI: 0.60, 0.88). Pathologists were initially in disagreement over 20 cases (17.7%) with regard to METAVIR fibrosis stage and for 21 cases (18.6%) with regard to necroinflammatory activity. The median time between hepatic biopsy and MR imaging was 23 days (range, 1–57 days).

Seventy-three patients (64.6%) had mild to no hepatic fibrosis ( $\leq$ F1), 40 (35.4%) had substantial fibrosis ( $\geq$ F2), 95 (84.1%) had non-advanced hepatic fibrosis ( $\leq$ F2), and 18 (15.9%) had advanced fibrosis or cirrhosis ( $\geq$ F3, Table 1). The median hepatic fat content was 3.6% (range, 0%–47.80%; IQR, 1.85%–7.10%). A significant moderate

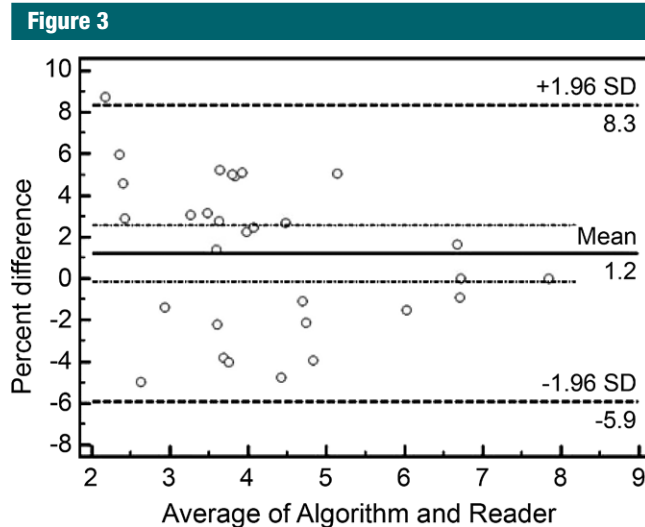


**Figure 3:** Bland-Altman plot used to compare the stiffness measurements from the reader and the automated algorithm. The 95% confidence limits of the bias are shown as two dotted lines. *SD* = standard deviation.

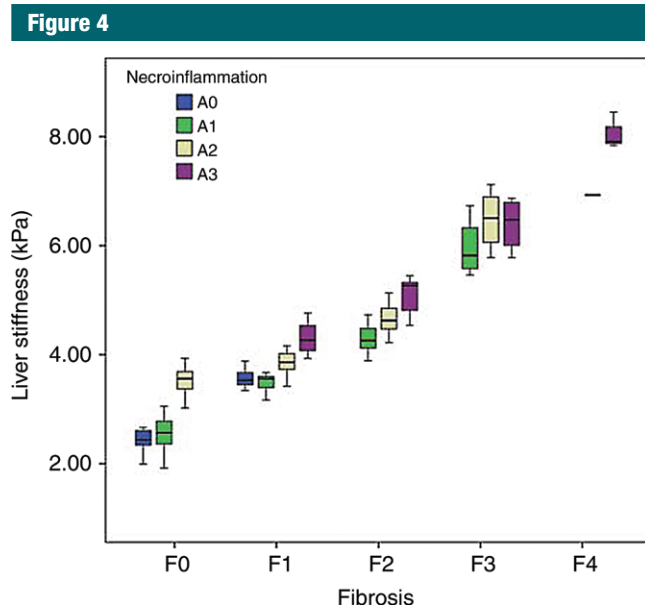


**Figure 4:** Box and whisker plot depicts hepatic stiffness according to fibrosis stage and necroinflammation grade. The boxes indicate the lower and upper quartiles for each group, and the dark horizontal line in the middle of the box is the median (50%) percentile. The whiskers are the lowest and highest values in distribution.

correlation was observed between the fibrosis stage and necroinflammation grade ( $r = 0.423$ ,  $P < .001$ ). A significant weak correlation was observed between the necroinflammation grade

and ALT or AST ( $r = 0.248$  and  $0.359$ , respectively [ $P < .01$ ]; Spearman correlation test) and between AST and fibrosis stage ( $r = 0.270$ ,  $P < .01$ ). AST/ALT ratio was also positively correlated

with both fibrosis stage ( $r = 0.464$ ,  $P < .01$ ) and necroinflammation grade ( $r = 0.217$ ,  $P < .05$ ).

#### Interobserver Agreement between Automated Algorithm and Reader

There was no significant difference between the measurements reported by the automated algorithm and the reader according to the intraclass correlation coefficient and the Bland-Altman test. Excellent agreement was seen with the intraclass correlation coefficient, equal to 0.996 (95% CI: 0.991, 0.998). No proportional bias or fixed bias was found for the two measurements; the mean bias was 1.2%, and the 95% limits of agreement were  $-5.9\%$  and  $8.3\%$  (Fig 3).

#### Hepatic Stiffness in Patients

Since the hepatic stiffness has a left-skewed distribution, the hepatic stiffness values within each group were reported as median values and IQR (Fig 4). The distribution of stiffness according to fibrosis stages and pathologic groups is shown in Table 2. After a natural log transform, the hepatic stiffness was distributed normally ( $P = .089$ ), and the variances were equal in these eight pathologic groups ( $P = .147$ ).

#### ROC Analyses and Diagnostic Performance for Predicting Fibrosis Stages and Necroinflammation Grades

The AUC values, optimal cutoff values, and respective diagnostic performance for hepatic stiffness are shown in Tables 3 and 4. The AUC shows that MR elastography has a high accuracy for diagnosis of fibrosis in all groups (values in all areas are higher than 0.9) and has a moderate diagnostic accuracy (areas between 0.8 and 0.9) for inflammation, as shown in Figure 5. All of the diagnostic performance measures for fibrosis are higher than 0.85, except for the negative predictive value for prediction of  $\geq F1$  fibrosis (0.677), with 3.61 kPa as the cutoff stiffness value. In patients with A0–A1, the optimal stiffness cutoffs for  $\geq F1$ ,  $\geq F2$ , and  $\geq F3$  were 3.05 kPa, 3.88 kPa, and 4.73 kPa, respectively; in patients with A2–A3, the optimal stiffness cutoffs

**Table 2**

**Liver Histologic Findings and Corresponding Hepatic Stiffness Measured with MR Elastography**

Fibrosis Stage	Median Hepatic Stiffness (kPa)	Necroinflammation Grade	Pathologic Group	No. of Patients	Median Hepatic Stiffness (kPa)
No fibrosis (F0)	2.66 (2.38, 3.32)	Mild (A0–1); severe (A2–3)	F0/A0–1; F0/A2–3	30; 13	2.51 (2.34, 2.66); 3.56 (3.38, 3.72)
Mild fibrosis (F1)	3.87 (3.71, 4.12)	Mild (A0–1); severe (A2–3)	F1/A0–1; F1/A2–3	12; 18	3.76 (3.60, 3.85); 4.05 (3.82, 4.22)
Moderate fibrosis (F2)	4.63 (4.26, 4.93)	Mild (A0–1); severe (A2–3)	F2/A0–1; F2/A2–3	9; 13	4.26 (4.08, 4.54); 4.85 (4.57, 5.27)
Advanced fibrosis (F3–4)	6.51 (5.78, 6.93)	Mild (A0–1); severe (A2–3)	F3–4/A0–1; F3–4/A2–3	6; 12	5.82 (5.58, 6.33); 6.80 (6.29, 7.48)

Note.—Data in parentheses are the 25th to 75th IQR percentiles.

**Table 3**

**Performance of Mean Hepatic Stiffness Measurements for the Prediction of METAVIR Fibrosis Stages according to Cutoff Values**

Parameter*	≥F1	≥F2	≥F3	F4
Cutoff stiffness (kPa)	3.61	4.07	5.45	6.87
AUC	0.961 (0.907, 0.989)	0.986 (0.944, 0.999)	1.000 (0.968, 1.000)	0.998 (0.963, 1.000)
Sensitivity	0.857 [60/70] (0.753, 0.929)	0.950 [38/40] (0.831, 0.994)	1.000 [18/18] (0.815, 1.000)	1.000 [4/4] (0.398, 1.000)
Specificity	0.907 [39/43] (0.779, 0.974)	0.945 [69/73] (0.866, 0.985)	1.000 [95/95] (0.962, 1.000)	0.991 [108/109] (0.950, 1.000)
Positive predictive value	0.965 (0.912, 0.991)	0.959 (0.896, 0.989)	1.000 (0.939, 1.000)	0.968 (0.685, 1.000)
Negative predictive value	0.677 (0.511, 0.819)	0.932 (0.789, 0.992)	1.000 (0.879, 1.000)	1.000 (0.852, 1.000)
Positive likelihood ratio	9.21 (8.00, 10.50)	17.30 (15.80, 19.00)	...	109.0 (107.0, 111.0)
Negative likelihood ratio	0.160 (0.05, 0.50)	0.050 (0.01, 0.30)	0.0	0.0

Note.—Numbers in parentheses indicate 95% CIs of the value. Numbers in brackets are raw data.  $P < .001$  for all comparisons.

\* For calculation of positive and negative predictive values, the prevalence for ≥F1, ≥F2, ≥F3, and F4 was 75.20%, 57.80%, 41.80%, and 21.50%, respectively.

**Table 4**

**Performance of Mean Stiffness for the Prediction of METAVIR Inflammatory Grades according to Cutoff Values**

Parameter*	≥A1	≥A2	A3
Cutoff stiffness (kPa)	3.53	3.24	4.16
AUC	0.806 (0.720, 0.875)	0.799 (0.714, 0.869)	0.900 (0.830, 0.949)
Sensitivity	0.680 [68/100] (0.579, 0.770)	0.982 [55/56] (0.904, 1.000)	0.947 [18/19] (0.740, 0.999)
Specificity	0.846 [11/13] (0.546, 0.981)	0.561 [32/57] (0.424, 0.693)	0.766 [72/94] (0.677, 0.847)
Positive predictive value	0.923 (0.777, 0.991)	0.631 (0.567, 0.731)	0.409 (0.283, 0.528)
Negative predictive value	0.492 (0.322, 0.610)	0.972 (0.841, 1.000)	0.988 (0.939, 1.000)
Positive likelihood ratio	4.42 (3.40, 5.80)	2.24 (1.80, 2.80)	4.05 (3.50, 4.70)
Negative likelihood ratio	0.38 (0.100, 1.40)	0.032 (0.004, 0.20)	0.069 (0.010, 0.50)

Note.—Numbers in parentheses indicate 95% CIs of the value. Numbers in brackets are raw data.  $P < .001$  for all comparisons.

\* For calculation of positive and negative predictive values, the prevalence for ≥A1, ≥A2, and A3 was 73.20%, 45.50%, and 14.60%, respectively.

for ≥F1, ≥F2, ≥F3, and F4 were 3.93 kPa, 4.31 kPa, 5.45 kPa, and 6.87 kPa, respectively.

**Influence of Necroinflammation Grade on Hepatic Stiffness**

According to univariate analysis, the log-transformed hepatic stiffness increased significantly with an increase

in fibrosis, necroinflammation, age, AST, and AST/ALT ratio ( $r = 0.914, 0.612, 0.212, 0.279, \text{ and } 0.416$ , respectively;  $P < .05$ ). No correlation was found between log-transformed hepatic stiffness and BMI, ALT, or hepatic steatosis ( $r = 0.016 [P = .866], 0.015 [P = 0.878], \text{ and } -0.058 [P = 0.532]$ , respectively). BMI, ALT, and

hepatic steatosis were then excluded from the multiple linear regression analysis. Although patient sex showed no difference in stiffness ( $P = .719$ ) according to the  $t$  test, it was still chosen to be a covariate because of previous studies (44,45). Multiple linear regression analysis showed that AST, AST/ALT ratio, and age could be excluded

**Figure 5**

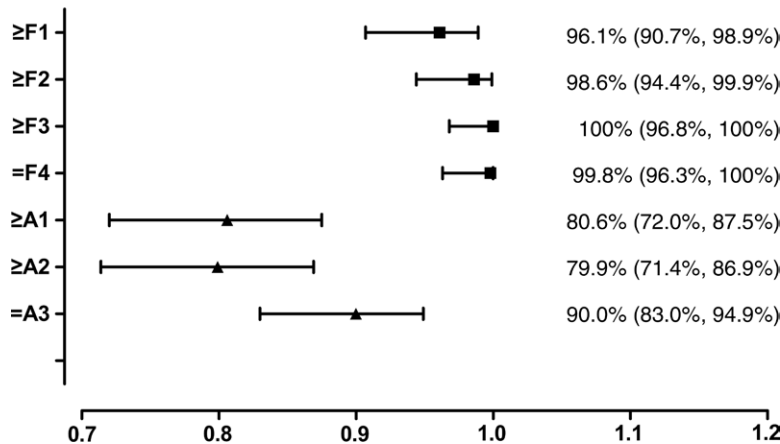


**Figure 5:** Forest plot shows pooled AUC values for MR elastography with 95% CIs (whiskers) for the prediction of hepatic fibrosis (grades ≥F1, ≥F2, ≥F3, and F4) and necroinflammatory grade (grades ≥A1, ≥A2, and A3).

**Table 5**

**Summary of the Pairwise Comparisons Analysis of Log-transformed Hepatic Stiffness between Pathologic Stages by Using the Bonferroni Post Hoc Multiple Comparisons Test**

Comparison	F0/A0-1	F0/A2-3	F1/A0-1	F1/A2-3	F2/A0-1	F2/A2-3	F3-4/A0-1
F0/A2-3	<.001	...	...	...	...	...	...
F1/A0-1	<.001	>.99*	...	...	...	...	...
F1/A2-3	<.001	.048	.045	...	...	...	...
F2/A0-1	<.001	<.001	<.001	.486*	...	...	...
F2/A2-3	<.001	<.001	<.001	<.001	.056*	...	...
F3-4/A0-1	<.001	<.001	<.001	<.001	<.001	<.001	...
F3-4/A2-3	<.001	<.001	<.001	<.001	<.001	.001	.069*

\* Log-transformed hepatic stiffness differences were found among all paired groups, except for group F0/A2-3 and F1/A0-1, group F1/A2-3 and F2/A0-1, group F2/A2-3 and F2/A0-1, and group F3/A0-1 and F3/A2-3.

as influences on the stiffness measurement, as approximately 89.9% of the total variability in hepatic stiffness values could be explained by three variables in this model (adjusted  $R^2 = 0.899$ ,  $F = 333.001$ ,  $P < .001$ ). Fibrosis stage, necroinflammation grade, and patient sex were the independent factors that contributed to hepatic stiffness ( $\beta = 0.799$  [ $P < .001$ ],  $0.277$  [ $P < .001$ ], and  $0.070$  [ $P = .033$ ], respectively).

Hepatic parenchyma with moderate to severe chronic hepatitis and without fibrosis (F0/A2-3) had a higher stiffness than that of tissue with mild to

no inflammation and no fibrosis (F0/A0-1) ( $P < .001$ , Table 5) but had a stiffness similar to that of tissue, with mild fibrosis and mild to no inflammation (F1/A0-1) ( $P > .99$ ). Likewise, livers with mild fibrosis and moderate to severe inflammation (F1/A2-3) had higher stiffness than tissue with mild fibrosis and mild to no inflammation (F1/A0-1,  $P = .045$ ) but had stiffness similar to tissue with moderate fibrosis and mild to no inflammation (F2/A0-1,  $P = .486$ ). However, the ALT and AST failed to show any statistical differences between adjacent pathologic groups (ALT,  $P = .008-.826$ ; AST, all  $P > .0018$ ).

**Discussion**

In this study, we used an automated stiffness measurement algorithm that can provide results comparable to those obtained by a trained reader of MR elastography data. The AUC showed that MR elastography had a high accuracy for diagnosis of fibrosis in all groups (AUC > 0.9). Multiple linear regression analysis showed that fibrosis stage, necroinflammation grade, and patient sex were independent factors that contributed to hepatic stiffness ( $\beta = 0.799$ ,  $0.277$ , and  $0.070$ , respectively;  $P < .05$ ). MR elastography cannot be used to distinguish between the stiffness of hepatic parenchyma with F0/A2-3 versus F1/A0-1 and F1/A2-3 versus F2/A0-1 classifications ( $P > .99$  and  $0.486$ , respectively), indicating that chronic hepatitis might be a confounding factor that causes an overestimation of true fibrosis stage in patients with  $\leq F2$  fibrosis.

Consistent with the meta-analysis from a previous study of MR elastography that showed AUCs of 0.95, 0.98, 0.98, and 0.99 for prediction of  $\geq F1$ ,  $\geq F2$ ,  $\geq F3$ , and  $\geq F4$  fibrosis stages (46), respectively, MR elastography in our study had a similarly high diagnostic accuracy for hepatic fibrosis in chronic HBV infection. MR elastography has previously been shown to have good diagnostic performance with regard to fibrosis staging in a Caucasian population with chronic HCV infection. We have now confirmed that it is also a good tool for Asian patients with chronic HBV infection. These results are in agreement with several smaller prior studies in Asian populations (26,27,47,48). The AUC for distinguishing the absence of fibrosis (F0) from fibrosis (F1-F4) in our study was 0.961, which is slightly lower than that in two of the other studies (0.98-0.99) (26,27). The cutoff value is 3.61 kPa, which is higher than that in other studies (2.40-2.93 kPa) (19-21). This high cutoff has a lower negative predictive value (0.677), indicating that the test would have a greater chance to cause misclassification of a case of F1 as being F0. In our study, the pathologic data were not distributed evenly,



with 95 patients (84.1%) who had non-advanced hepatic fibrosis ( $\leq$ F2) and 82 patients who had chronic hepatitis (72.6%) showing more severe inflammation than that reported in the literature (9,26,30). As suggested in some previous MR elastography and transient elastography studies, hepatic stiffness is likely to increase because of chronic hepatitis infection before the development of fibrosis (9,30). In cases of  $\leq$ F2 fibrosis, grade A2–A3 inflammation will significantly increase hepatic stiffness, leading to the absence of a significant difference with the next fibrosis stage. We hypothesize that the onset of hepatic injury causes the accumulation of interstitial liquid and inflammatory infiltration. This may lead to increased intrinsic stress, resulting in an increase in hepatic stiffness (49,50).

Compared with chronic HCV infection and alcoholic cirrhosis, the amount of fibrosis is lower in chronic HBV infection for patients with  $\leq$ F2 fibrosis, mainly because of the decreased perisinusoidal fibrosis (8). This histologic difference implies lower hepatic stiffness in chronic HBV infection than in chronic HCV infection (7,8,51). The smaller amount of fibrosis and the greater variability of inflammation in chronic HBV infection might partially explain the controversy of the stiffness cutoffs for patients with chronic HBV infection and chronic HCV infection at the same fibrotic level in different transient elastography studies (7,52). Several studies with single disease origins like chronic HBV infection, chronic HCV infection, and nonalcoholic steatohepatitis have emerged (26–29,53,54). From the MR elastography study reported by Venkatesh et al in patients with chronic HBV infection (26), the cutoff values were higher than those reported in patients with chronic HCV infection (20,27) for the F1 and F2 groups, but they were lower for F3 and F4. The corresponding cutoffs were 2.74, 3.2, 3.7, and 4.33 kPa in that study, which are lower at each stage of fibrosis than in our study. We speculate that most of their cases (54 of 63 cases, 85.7%) had mild to no inflammation (grades A0–1), which contributed to lower stiffness.

For identification of  $\geq$ F2 and  $\geq$ F3 stages, our cutoffs (4.07 kPa and 5.45 kPa, respectively) were within the literature ranges with different disease origins (3.19–5.37 kPa for  $\geq$ F2 and 4.21–6.47 kPa for  $\geq$ F3). Our data had a cutoff value to identify the presence of cirrhosis (F4) that was higher than that in the literature (6.87 kPa vs 5.97–6.47 kPa) (9,19–21,27), possibly because only a few patients with advanced fibrosis were included in the current study. Studies showed that hepatic stiffness might also be useful to show the real hepatic fibrosis after the acute flare-up of chronic HBV infection was controlled or stabilized with the return of evaluated ALT and AST (20,55). However, the ALT, AST, and AST/ALT ratio in the current study were only weakly correlated with necroinflammation grade and failed to show statistical differences between adjacent pathologic groups. It is thus still unclear whether the serum hepatic enzyme levels (ALT and AST) could be useful as a means to adjust or normalize for inflammatory severity.

Our study has several limitations. First, the histologic findings were not uniformly distributed as to degree of fibrosis, and there were more cases with the lower fibrotic stages. Second, it is better to compare the performance of MR elastography for both chronic HBV and chronic HCV infection directly by using the same imager type, imaging protocol, and processing and analysis tools. Even within the cohort of patients in this study, the imaging protocol was changed, which could have introduced some variation in the results. Third, the current histologic reference standards for evaluation of hepatic fibrosis are only semiquantitative. Taking a quantitative approach, such as morphometric analysis (8), to evaluate collagen concentrations and the distribution of hepatic fibrosis may be more beneficial in establishing the relationship of MR elastography stiffness with the amount of fibrosis than the use of fibrotic stage alone. Finally, the cutoffs reported were derived from this study and were likely to be overstated. The present results need to be validated independently in further studies.

In conclusion, we showed that the diagnostic performance of MR elastography is promising for use in clinical practice to evaluate fibrosis and cirrhosis in Asian patients with chronic HBV infection, although dual cutoff values or different cutoff values in patients with advanced inflammation might be needed on the basis of pathologic necroinflammation grade obtained from hepatic biopsy instead of these serum markers. Both hepatic fibrosis and necroinflammation are independent factors that affect hepatic stiffness. For the diagnosis of nonadvanced fibrosis ( $F \leq 2$ ), inflammation should be taken into account as a confounding factor that increases hepatic stiffness, potentially causing overestimation of the real fibrosis stage.

**Disclosures of Conflicts of Interest:** **Y.S.** No relevant conflicts of interest to disclose. **Q.G.** No relevant conflicts of interest to disclose. **E.X.** No relevant conflicts of interest to disclose. **B.D.** Financial activities related to the present article: author and Mayo Clinic have patents and receive royalties for MR elastography. Financial activities not related to the present article: none to disclose. Other relationships: none to disclose. **K.J.G.** Financial activities related to the present article: author and Mayo Clinic have patents and receive royalties for MR elastography, and the author has stock options in Resoundant, a Mayo Clinic company. Financial activities not related to the present article: none to disclose. Other relationships: none to disclose. **Q.L.** No relevant conflicts of interest to disclose. **J.L.** No relevant conflicts of interest to disclose. **R.L.E.** Financial activities related to the present article: author is CEO of Resoundant, a Mayo Clinic company; author and Mayo Clinic have patents and receive royalties for MR elastography. Financial activities not related to the present article: none to disclose. Other relationships: none to disclose.

## References

- Ott JJ, Stevens GA, Groeger J, Wiersma ST. Global epidemiology of hepatitis B virus infection: new estimates of age-specific HBsAg seroprevalence and endemicity. *Vaccine* 2012;30(12):2212–2219.
- Mohd Hanafiah K, Groeger J, Flaxman AD, Wiersma ST. Global epidemiology of hepatitis C virus infection: new estimates of age-specific antibody to HCV seroprevalence. *Hepatology* 2013;57(4):1333–1342.
- European Association for the Study of the Liver. EASL clinical practice guidelines: Management of chronic hepatitis B virus infection. *J Hepatol* 2012;57(1):167–185.

4. Fattovich G, Olivari N, Pasino M, D'Onofrio M, Martone E, Donato F. Long-term outcome of chronic hepatitis B in Caucasian patients: mortality after 25 years. *Gut* 2008;57(1):84-90.
5. Fattovich G, Stroffolini T, Zagni I, Donato F. Hepatocellular carcinoma in cirrhosis: incidence and risk factors. *Gastroenterology* 2004;127(5,Suppl 1):S35-S50.
6. Bosch FX, Ribes J, Cléries R, Díaz M. Epidemiology of hepatocellular carcinoma. *Clin Liver Dis* 2005;9(2):191-211, v.
7. Verveer C, Zondervan PE, ten Kate FJ, Hansen BE, Janssen HL, de Knecht RJ. Evaluation of transient elastography for fibrosis assessment compared with large biopsies in chronic hepatitis B and C. *Liver Int* 2012;32(4):622-628.
8. Sturm N, Marlu A, Arvers P, Zarski JP, Leroy V. Comparative assessment of liver fibrosis by computerized morphometry in naïve patients with chronic hepatitis B and C. *Liver Int* 2013;33(3):428-438.
9. Wang Y, Ganger DR, Levitsky J, et al. Assessment of chronic hepatitis and fibrosis: comparison of MR elastography and diffusion-weighted imaging. *AJR Am J Roentgenol* 2011;196(3):553-561.
10. Myers RP, Tainturier MH, Ratziu V, et al. Prediction of liver histological lesions with biochemical markers in patients with chronic hepatitis B. *J Hepatol* 2003;39(2):222-230.
11. Wai CT, Cheng CL, Wee A, et al. Non-invasive models for predicting histology in patients with chronic hepatitis B. *Liver Int* 2006;26(6):666-672.
12. Wai CT, Greenon JK, Fontana RJ, et al. A simple noninvasive index can predict both significant fibrosis and cirrhosis in patients with chronic hepatitis C. *Hepatology* 2003;38(2):518-526.
13. Castera L. Noninvasive methods to assess liver disease in patients with hepatitis B or C. *Gastroenterology* 2012;142(6):1293-1302, e4.
14. Rockey DC, Bissell DM. Noninvasive measures of liver fibrosis. *Hepatology* 2006;43(2 Suppl 1):S113-S120.
15. Chan HL, Wong GL, Choi PC, et al. Alanine aminotransferase-based algorithms of liver stiffness measurement by transient elastography (Fibroscan) for liver fibrosis in chronic hepatitis B. *J Viral Hepat* 2009;16(1):36-44.
16. Wong GL, Wong VW, Choi PC, et al. Assessment of fibrosis by transient elastography compared with liver biopsy and morphometry in chronic liver diseases. *Clin Gastroenterol Hepatol* 2008;6(9):1027-1035.
17. Castéra L, Foucher J, Bernard PH, et al. Pitfalls of liver stiffness measurement: a 5-year prospective study of 13,369 examinations. *Hepatology* 2010;51(3):828-835.
18. Friedrich-Rust M, Nierhoff J, Lupsor M, et al. Performance of Acoustic Radiation Force Impulse imaging for the staging of liver fibrosis: a pooled meta-analysis. *J Viral Hepat* 2012;19(2):e212-e219.
19. Yin M, Talwalkar JA, Glaser KJ, et al. Assessment of hepatic fibrosis with magnetic resonance elastography. *Clin Gastroenterol Hepatol* 2007;5(10):1207-1213, e2.
20. Huwart L, Sempoux C, Salameh N, et al. Liver fibrosis: noninvasive assessment with MR elastography versus aspartate aminotransferase-to-platelet ratio index. *Radiology* 2007;245(2):458-466.
21. Huwart L, Sempoux C, Vicaut E, et al. Magnetic resonance elastography for the noninvasive staging of liver fibrosis. *Gastroenterology* 2008;135(1):32-40.
22. Asbach P, Klatt D, Schlosser B, et al. Viscoelasticity-based staging of hepatic fibrosis with multifrequency MR elastography. *Radiology* 2010;257(1):80-86.
23. Yin M, Chen J, Glaser KJ, Talwalkar JA, Ehman RL. Abdominal magnetic resonance elastography. *Top Magn Reson Imaging* 2009;20(2):79-87.
24. Rustogi R, Horowitz J, Harmath C, et al. Accuracy of MR elastography and anatomic MR imaging features in the diagnosis of severe hepatic fibrosis and cirrhosis. *J Magn Reson Imaging* 2012;35(6):1356-1364.
25. Nedredal GI, Yin M, McKenzie T, et al. Portal hypertension correlates with splenic stiffness as measured with MR elastography. *J Magn Reson Imaging* 2011;34(1):79-87.
26. Venkatesh SK, Wang G, Lim SG, Wee A. Magnetic resonance elastography for the detection and staging of liver fibrosis in chronic hepatitis B. *Eur Radiol* 2014;24(1):70-78.
27. Ichikawa S, Motosugi U, Ichikawa T, et al. Magnetic resonance elastography for staging liver fibrosis in chronic hepatitis C. *Magn Reson Med Sci* 2012;11(4):291-297.
28. Kamphues C, Klatt D, Bova R, et al. Viscoelasticity-based magnetic resonance elastography for the assessment of liver fibrosis in hepatitis C patients after liver transplantation. *Rofo* 2012;184(11):1013-1019.
29. Shire NJ, Yin M, Chen J, et al. Test-retest repeatability of MR elastography for noninvasive liver fibrosis assessment in hepatitis C. *J Magn Reson Imaging* 2011;34(4):947-955.
30. Cardoso AC, Carvalho-Filho RJ, Stern C, et al. Direct comparison of diagnostic performance of transient elastography in patients with chronic hepatitis B and chronic hepatitis C. *Liver Int* 2012;32(4):612-621.
31. Marcellin P, Ziolkowski M, Bedossa P, et al. Non-invasive assessment of liver fibrosis by stiffness measurement in patients with chronic hepatitis B. *Liver Int* 2009;29(2):242-247.
32. Chrysanthos NV, Papatheodoridis GV, Savvas S, et al. Aspartate aminotransferase to platelet ratio index for fibrosis evaluation in chronic viral hepatitis. *Eur J Gastroenterol Hepatol* 2006;18(4):389-396.
33. Manduca A, Oliphant TE, Dresner MA, et al. Magnetic resonance elastography: non-invasive mapping of tissue elasticity. *Med Image Anal* 2001;5(4):237-254.
34. Manduca A, Lake DS, Kruse SA, Ehman RL. Spatio-temporal directional filtering for improved inversion of MR elastography images. *Med Image Anal* 2003;7(4):465-473.
35. Dzyubak B, Glaser K, Yin M, et al. Automated liver stiffness measurements with magnetic resonance elastography. *J Magn Reson Imaging* 2013;38(2):371-379.
36. Bedossa P, Poinard T. An algorithm for the grading of activity in chronic hepatitis C. The METAVIR Cooperative Study Group. *Hepatology* 1996;24(2):289-293.
37. Theise ND. Liver biopsy assessment in chronic viral hepatitis: a personal, practical approach. *Mod Pathol* 2007;20(Suppl 1):S3-S14.
38. Intraobserver and interobserver variations in liver biopsy interpretation in patients with chronic hepatitis C. The French METAVIR Cooperative Study Group. *Hepatology* 1994;20(1 Pt 1):15-20.
39. Bland JM, Altman DG. Statistical methods for assessing agreement between two methods of clinical measurement. *Lancet* 1986;1(8476):307-310.
40. Ludbrook J. Statistical techniques for comparing measurers and methods of measurement: a critical review. *Clin Exp Pharmacol Physiol* 2002;29(7):527-536.
41. Kundel HL, Polansky M. Measurement of observer agreement. *Radiology* 2003;228(2):303-308.
42. Jaeschke R, Guyatt GH, Sackett DL. Users' guides to the medical literature. III. How to use an article about a diagnostic test. B. What are the results and will they help me in caring for my patients? The Evidence-Based Medicine Working Group. *JAMA* 1994;271(9):703-707.

43. Fritz JM, Wainner RS. Examining diagnostic tests: an evidence-based perspective. *Phys Ther* 2001;81(9):1546–1564.
44. Roulot D, Czernichow S, Le Clésiau H, Costes JL, Vergnaud AC, Beaugrand M. Liver stiffness values in apparently healthy subjects: influence of gender and metabolic syndrome. *J Hepatol* 2008;48(4):606–613.
45. Mannelli L, Godfrey E, Joubert I, et al. MR elastography: spleen stiffness measurements in healthy volunteers—preliminary experience. *AJR Am J Roentgenol* 2010;195(2):387–392.
46. Wang QB, Zhu H, Liu HL, Zhang B. Performance of magnetic resonance elastography and diffusion-weighted imaging for the staging of hepatic fibrosis: a meta-analysis. *Hepatology* 2012;56(1):239–247.
47. Kim BH, Lee JM, Lee YJ, et al. MR elastography for noninvasive assessment of hepatic fibrosis: experience from a tertiary center in Asia. *J Magn Reson Imaging* 2011;34(5):1110–1116.
48. Swets JA. Measuring the accuracy of diagnostic systems. *Science* 1988;240(4857):1285–1293.
49. Yin M, Talwalkar JA, Glaser KJ, et al. Dynamic postprandial hepatic stiffness augmentation assessed with MR elastography in patients with chronic liver disease. *AJR Am J Roentgenol* 2011;197(1):64–70.
50. Hines CD, Bley TA, Lindstrom MJ, Reeder SB. Repeatability of magnetic resonance elastography for quantification of hepatic stiffness. *J Magn Reson Imaging* 2010;31(3):725–731.
51. Fraquelli M, Rigamonti C, Casazza G, et al. Etiology-related determinants of liver stiffness values in chronic viral hepatitis B or C. *J Hepatol* 2011;54(4):621–628.
52. Oliveri F, Coco B, Ciccorossi P, et al. Liver stiffness in the hepatitis B virus carrier: a non-invasive marker of liver disease influenced by the pattern of transaminases. *World J Gastroenterol* 2008;14(40):6154–6162.
53. Chen J, Talwalkar JA, Yin M, Glaser KJ, Sanderson SO, Ehman RL. Early detection of nonalcoholic steatohepatitis in patients with nonalcoholic fatty liver disease by using MR elastography. *Radiology* 2011;259(3):749–756.
54. Bensamoun SF, Leclerc GE, Debernard L, et al. Cutoff values for alcoholic liver fibrosis using magnetic resonance elastography technique. *Alcohol Clin Exp Res* 2013;37(5):811–817.
55. Venkatesh SK, Yin M, Ehman RL. Magnetic resonance elastography of liver: clinical applications. *J Comput Assist Tomogr* 2013;37(6):887–896.